論文 The Finite Element with Inner Linkage Rods

Junichiro NIWA*[1], Guo-xiong YU*[2], and Tada-aki TANABE*[3]

ABSTRACT: In this paper, a new technique for modeling the crack behaviors of concrete structures is described, where the softening band (crack) inside the element is represented by two rods whose behaviors follow the fracture-oriented constitutive relations. This new method, like the discrete model, can reflect the localized nature of cracking and at the same time can easily be implemented into the commonly used finite element program to analyze any arbitrary concrete structures. In this paper, examples with different kinds of meshes are used to show the objectivity of this method.
KEYWORDS: finite element, rod element, discrete model, fracture energy, objectivity, localization.

1. INTRODUCTION

Up to now, to describe the cracking of concrete, two different approaches are often used: the discrete approach and the smeared approach. However, there are still some problems existing. The discrete approach is attractive physically, as it reflects the localized nature of cracking, but its numerical implementation is hampered by the need for letting the cracks follow the element boundaries, thereby requiring the introduction of additional nodal points or rearrangement of the original mesh. Smeared model have been widely used in finite element analysis. However, for some problems, as pointed out by Shirai,N.[1] and Rots [2], it is doubtful that the smeared model can suitably simulate a localization of fracture and unloading behaviors in surrounding region for the reason of stress locking.

In view of this, in this paper, a way is developed to correctly reflect the localized nature of crack and at the same time to be easily implemented into finite element program to analyze arbitrary concrete structures. Basically, this method uses the discrete model but overcomes its disadvantage. So, like the discrete model, the problem of stress locking does not exist in this method.

2. FINITE ELEMENT WITH INNER LINKAGE RODS ELEMENT

In this research, the rod linkage element is used to represent the localized crack and to link the unloading concretes on two sides of this crack. This rod linkage element is composed of two rods, which follow the fracture-oriented constitutive relation. **Fig.**1 shows the rod linkage rods element. Rod A is the rod describing the tension behavior of the crack and Rod B the shear slip behavior of the crack. **Fig.**2(a) and **Fig.**2(b) show the finite element with inner linkage rods when single crack occurs.

*1 Department of Civil Engineering, Nagoya University DR,Member of JCI
*2 Department of Civil Engineering, Nagoya University, Member of JCI
*3 Department of Civil Engineering, Nagoya University, DR,Member of JCI

The procedure to implement this kind of element can be described as follows:

1. For every element in the mesh the maximum principle stress at the center of the element is calculated out. The stress state at the center of the element can simply obtained by averaging the stresses at 2×2 Gauss points when 4-node isoparametric elements are used, or directly using one-point integration rule [3]. This calculation is repeated at every step of the solution process until the maximum principle stress is equal to or larger than the tensile strength of the material, that means that a crack occurs through the center of the element.

2. From this point on, the finite element where the crack occurs, is replaced by the finite element with inner linkage rods that is mentioned above. The crack with angle α , shown in **Fig.**2(a) and **Fig.**2(b), is normal to the maximum principle stress. The crack length L can be calculated out and the section area of Rod A and Rod B are equal to $Lt/2$, where t is the thickness of this element. The inner freedom related to points a, b, c and d can be eliminated at element level by means of static condensation, by this way the stiffness matrix related with points 1, 2, 3 and 4 can be obtained.

When the crack goes through or near the diagonal nodes of the element, the finite element with inner linkage rods shown in **Fig.**2(b) should be used, otherwise the element shown in **Fig.**2(a) should be used for ensuring that the element has a good shape and good performance. To use this method to analyze concrete structures, the only thing to do is, first, making a subroutine using displacements control method to describe the nonlinear behaviors of the substructures (shown in **Figs.**2 (a)(b)), and then, implementing this subroutine into the common used finite element program.

3. FICTITIOUS CRACK MODEL

The fictitious crack model was first introduced by Hillerborg, et al. [4] and in its original form, it is a discrete approach. When the crack opens the stress is not assumed to fall to zero at once, but to decrease with increasing width, as shown in **Fig.**3. At the crack width w_1 the stress falls to zero. Energy dissipated D_t per unit crack area, is related to the area under the $\sigma - w$ curve of **Fig.**3, i.e.,

$$D_t = \int_0^{w_1} \sigma dW = G_f \qquad (1)$$

where G_f is the fracture energy, i.e., . the energy required to create a fully open crack plane of unite area, and w_1 is shown in **Fig.**3.

In the application of the fictitious model, the curve $\sigma(w)$ may be chosen in different ways. In the analysis of this paper, the curve shown in **Fig.**4 is used.

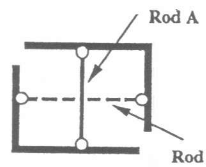

Figure 1: The rod linkage element

(a)

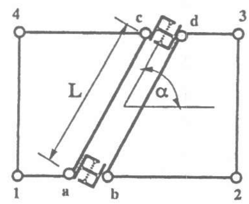

(b)

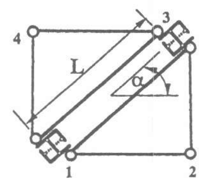

Figure 2: The element with inner linkage rods

4. ROD ELEMENT FOR SIMULATING THE TENSION BEHAVIOR OF THE CRACK

4.1 LOADING BEHAVIORS

Assuming the rod has the unit length, the loading stress-strain relation curve of Rod A can be shown by **Fig.**4. We assume the initial stiffness of the rod element $E_R = 100 \times E_c$, where E_c is the Young's modulus of the concrete, in order to make sure that before the crack occurs, the difference in displacements at two ends of the rod is small enough.

$$\varepsilon_p = \frac{f_t}{E_R} \qquad \varepsilon_1 = 0.75\frac{G_f}{f_t} \qquad \varepsilon_2 = 5\frac{G_f}{f_t} \tag{2}$$

$$\sigma = \begin{cases} E_R\varepsilon & 0 < \varepsilon \leq \varepsilon_p \\ f_t - \dfrac{0.75 f_t(\varepsilon - \varepsilon_p)}{\varepsilon_1 - \varepsilon_p} & \varepsilon_p < \varepsilon \leq \varepsilon_1 \\ \dfrac{f_t}{4} - \dfrac{f_t(\varepsilon - \varepsilon_1)}{4(\varepsilon_2 - \varepsilon_1)} & \varepsilon_1 < \varepsilon \leq \varepsilon_2 \\ 0 & \varepsilon_2 < \varepsilon \end{cases} \tag{3}$$

$$E = \begin{cases} E_R & 0 < \varepsilon \leq \varepsilon_p \\ -\dfrac{0.75 f_t}{\varepsilon_1 - \varepsilon_p} & \varepsilon_p < \varepsilon \leq \varepsilon_1 \\ -\dfrac{f_t}{4(\varepsilon_2 - \varepsilon_1)} & \varepsilon_1 < \varepsilon \leq \varepsilon_2 \\ 0 & \varepsilon_2 < \varepsilon \end{cases} \tag{4}$$

where f_t is the tension strength of the concrete and G_f is the fracture energy of the concrete material.

4.2 UNLOADING AND RELOADING BEHAVIORS

In practice, it is also important to have realistic models for the closing and reopening of cracks, especially when the crack localization phenomenon occurs. Loading and unloading correspond to the strain increasing and decreasing situation in analysis.

Assume that at point $(\sigma_u, \varepsilon_u)$, $\varepsilon_p < \varepsilon_u < \varepsilon_2$, the unloading is detected, the path of unloading will follow the **Eq.(5)** as shown by **Fig.**5(a).

$$\sigma = \begin{cases} \dfrac{\sigma_u(\varepsilon - \beta\varepsilon_u)}{(1-\beta)\varepsilon_u} & \beta\varepsilon_u \leq \varepsilon \\ E_R(\varepsilon - \beta\varepsilon_u) & \varepsilon < \beta\varepsilon \end{cases} \tag{5}$$

where E_R has the same meaning as in **Eq.(2)**. β is the material parameter, if β is chosen as zero, this corresponds to fully recoverable crack width, whereas, $\beta = 1$ corresponds to total irrecoverable crack width as shown in **Fig.**5(c). In this study, β is chosen to be 0.

If $\varepsilon_u > \varepsilon_2$ the unloading and reloading path follow **Fig.**5(b).

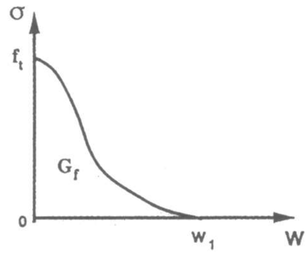

Figure 3:
The fictitous crack model of Hillerborg

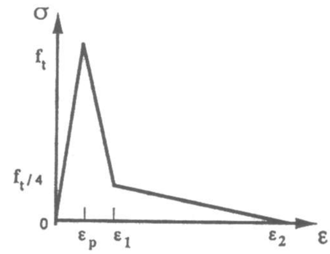

Figure 4:
The stress-strain curve inner linkage rod A

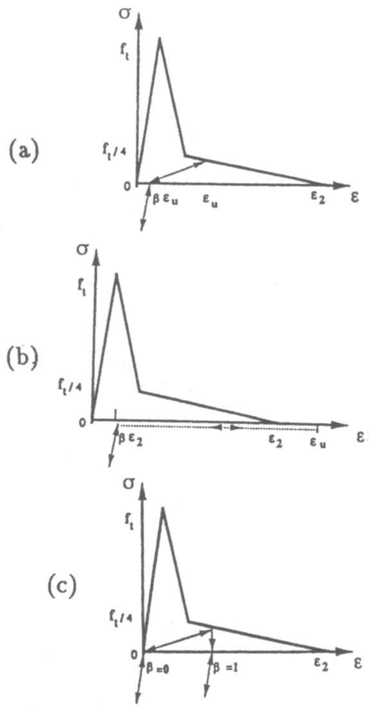

Figure 5:
The unloading behaviors of rod A

5. ROD ELEMENT FOR SIMULATING THE SHEAR SLIP BEHAVIOR OF THE CRACK

The original fictitious crack model considers only the behavior of a crack loaded normal to the crack plane. In reality, crack planes are often exposed to shear. From the experimental observation [5], when the crack occurs, the tangential crack displacement w_t depends on both the shear stress and the normal crack displacement w_n. Note that both the Rod A and Rod B have the unit length, we can write

$$\varepsilon_t = f(\tau, \varepsilon_n) \tag{6}$$

where ε_t is the strain of Rod B, and τ is the stress of Rod B and ε_n is the strain of Rod A.

For **Eq.(6)**, a simple form as in Ref.[6] is used as

$$\varepsilon_t = \frac{\varepsilon_n}{G_s}\tau \tag{7}$$

In order to fit with the experiment result [5], G_s is taken as 3.8 MPa.

6. TANGENTIAL STIFFNESS MATRIX FOR ROD ELEMENT

Fig.6 shows a rod element in global coordinates X-Y, with angle θ to X axis. The stiffness matrix of the rod with reference to the global coordinate will be

$$\begin{aligned} [K] &= A_s \int_0^L [B]\, E\, [B]^T\, dx \\ &= \frac{A_s E}{L} \begin{bmatrix} c^2 & sc & -c^2 & -sc \\ -sc & s^2 & -sc & -s^2 \\ -c^2 & -sc & c^2 & sc \\ -sc & -c^2 & -sc & s^2 \end{bmatrix} \end{aligned} \tag{8}$$

where E is the Young's modulus of the rod, while A_s is the section area of the rod and $c = cos\theta$, $s = sin\theta$.

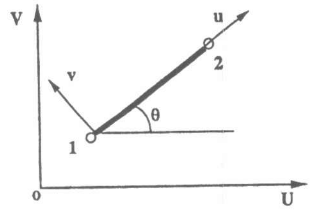

Figure 6:
Displacement of the rod element

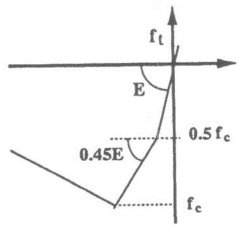

Figure 7:
The uniaxial stress-strain curve

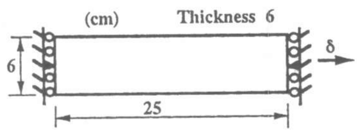

Figure 8:
Dimension and boundary condition of example 1

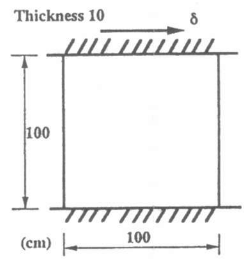

Figure 9:
Dimension and boundary condition for example 2

7. NUMERICAL EXAMPLE

The problems analyzed below are assumed to be the plane stress problems. Drucker-Prager type constitutive equation with the uniaxial stress-strain curve in **Fig.**7 is employed to describe the compressive behaviors of concrete.

For each example, with respect to different load levels, the crack patterns, which indicate the orientation and width of the cracks, will be shown. When the width of the crack is equal to

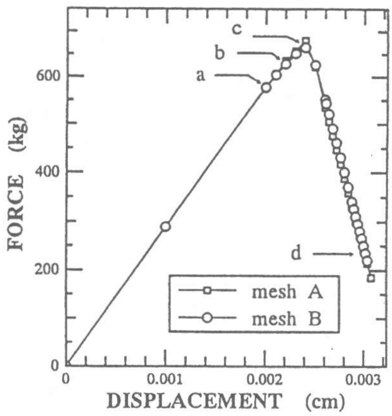

Figure 10: Load-displacement curves for example 1

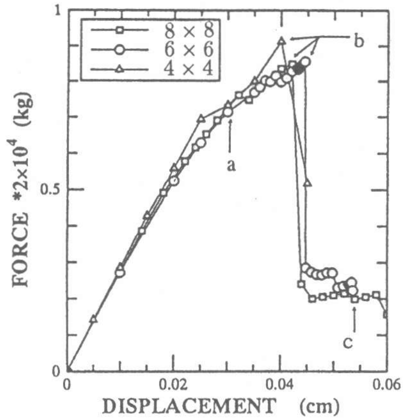

Figure 11: Load-displacement curves for example 2

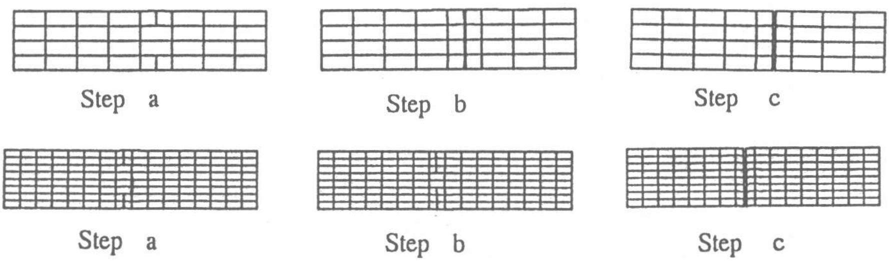

Figure 12: Crack pattern for example 1

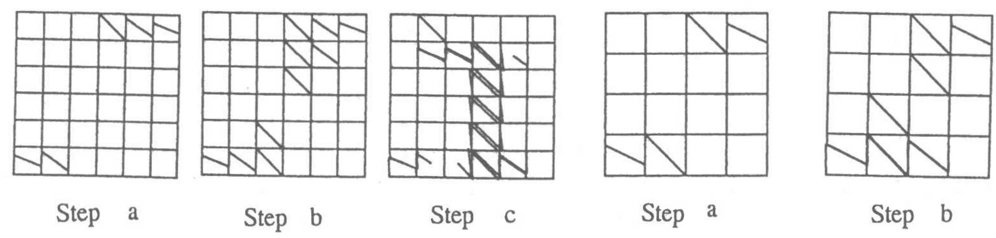

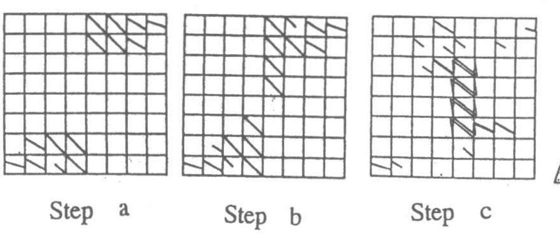

Figure 13: Crack patterns for example 2

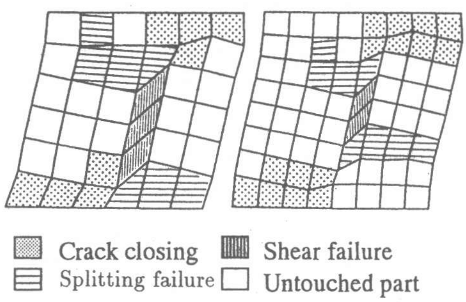

Figure 14: Failure modes for example 2

zero(this means the crack has closed), this crack will not be drawn. From these crack patterns the procedures of opening and closing of the crack can be seen clearly.

The first example is a plain concrete prism subjected to prescribed uniform displacements at both ends. The dimension and the supporting condition are shown in **Fig.**8. The material properties are as follows: $E = 2.1 \times 10^5 kgf/cm^2$, $f_t = 26.3kgf/cm^2$, $f_c = 190kgf/cm^2$ and $G_f = 100N/m = 0.1kg/cm$. Two kinds of mesh 16×8 and 8×4 are used to demonstrate the objectivity of this method and shown in **Fig.**12. The imperfection elements, are embedded in the center of two sides of the bar. The imperfection element has the same material properties as the other elements but the thickness is reduced to $3cm$. The load-displacement curves are shown in **Fig.**10 with two kinds of mesh used. The results are shown in **Fig.**12 depicting the crack patterns at different load levels. The objectivity of this method can be demonstrated by **Fig.**10.

The second example is a pain concrete wall subjected to shear displacement as illustrated in **Fig.**9. A series of computation were carried out with uniform design of finite element meshes with increasing refinement(4×4, 6×6 and 8×8). The progressive development of crack with regard to different stages is depicted in **Fig.**13. The inherent objectivity of the numerical results with respect to the choice of the finite element mesh is reasonably well demonstrated in **Fig.**11. In **Fig.**13, it is well demonstrated the crack opening and closing procedure, and at step c the structure finally fails with a major failure zone. The analytical failure modes are shown by **Fig.**14.

8. CONCLUSIONS

In this paper, a new technique for modeling the crack behaviors of concrete structures is presented, where the crack inside the element is represented by two rod elements whose behavior is based on the fracture-oriented constitutive relations. It has been confirmed by the numerical results in this paper that this new method is objective with respect to the choice of the element size, that it can reflect the localized nature of cracking and that it can be easily implemented into the commonly used finite element programs to analyze any arbitrary concrete structures.

REFERENCE

1) Shirai,N.,"JCI Round Robin Analysis in Size Effect in Concrete Structures," JCI International Workshop on Size Effect in concrete Structures, Sendai, Japan, Oct., 1993, pp.247-270.

2) Rots, J.G., "Computational Modeling of Concrete Fracture," Heron, Vol.34, No.1, 1988, p.59.

3) Yu, G.X. and Tanabe, T., "One-point Integration Rule in Nonlinear Problems," Proceedings of the Japan Concrete Institute, Vol.16, No.2, 1994, pp.117-223.

4) Hillerborg,A., Modeer,M. and Peterson,P.E., "Analysis of Crack Formation and Crack Growth in Concrete by Means of Fracture Mechanics and Finite Element," Cement and Concrete Research, Vol.6, 1976, pp.773-783.

5) Paulay,T. and Loeber,P.S.,"Shear Transfer by Aggregate Interlock." Shear in Reinforced concrete, Special Publ.,SP-42, 1, Amer. Concrete Institute, Detroit, Mich., 1974, pp.1–15.

6) Dahoblom,O. and Ottosen,N.S., "Smeared Crack Analysis Using Generalized Fictitious Crack Models." ASCE Journal of Engineering Mechanics, Vol.116, No.1, Jan., 1990, pp.55-76.